Proceedings of the Combustion Institute, Volume 29, 2002/pp. 407–414

MODELING BIOMASS DEVOLATILIZATION USING THE CHEMICAL PERCOLATION DEVOLATILIZATION MODEL FOR THE MAIN COMPONENTS

CHANGDONG SHENG AND J. L. T. AZEVEDO
Mechanical Engineering Department
Instituto Superior Técnico
Av. Rovisco Pais
1049-001 Lisbon, Portugal

Devolatilization plays a significant role in biomass combustion processes, and it depends on the biomass form and composition. In the present work, a general model is developed for the devolatilization of biomass under different conditions, particularly under high heating rate (up to 1000 K/s) and high temperature (up to 1400 K). The model was developed extending the chemical percolation devolatilization model from coal to the three main biomass components, that is, cellulose, hemicellulose, and lignin, on the basis of their specific chemical structure and behavior. The model formulation was kept with the same reaction scheme and multimechanisms. The modifications were performed on the structural parameters and reaction kinetics considering a chain structure for the components. The devolatilization of the whole biomass was modeled as the superposition of the independent kinetics of the major components. The structural and kinetic parameters were fixed for the components, while the only fuel-specific input, the mass fraction of the components, can be calculated with a proposed correlation as a function of the conventional proximate and ultimate analyses. Comparisons to the measurements show that the model has been successfully applied to the devolatilization of various biomass types and can reasonably represent the yields of tar, light gases, and char, when considering side chains from tars as secondary products.

Introduction

The environmental and political concern related to CO_2 emission has increased the interest of directly burning or cofiring biomass for electricity generation. Compared with coals, biomass is characterized by higher volatile content and a rapid decomposition starting at very low temperatures (down to 160–300 °C). Devolatilization has a significant effect on the combustion process and consequently on the design and operation of the combustion systems of these fuels [1], which has motivated extensive studies to understand its mechanisms and characteristics, as summarized in several reviews [1–6].

Despite its diverse forms and composition, biomass is generally a chemical mixture of polymer components, that is, cellulose, hemicellulose, and lignin, as well as extractives [2,3]. The variation of chemical composition results in changes in the devolatilization characteristics. Therefore, a general biomass devolatilization model covering various biomass types and different conditions would be a valuable tool for design and operation engineers and also the aim of modeling researchers. Much work has been done to model the devolatilization of biomass as well as its major components, as reported in papers on biomass [2,6–13], cellulose [7–9,14–18], and lignin [8,9,19–22] and also summarized in reviews [6,17,23,24]. Many kinetic models have been proposed to describe biomass devolatilization [23]. However, the kinetic models were often proposed based on experiments using specific species or components in specific reaction conditions. Therefore, the empirical models developed cannot cover the various mechanisms involved in biomass devolatilization and are only strictly applicable to the samples considered. For example, under conditions that minimize vapor-solid interactions and heat transfer effect, single stage first-order kinetic models can accurately represent cellulose devolatilization [24]. At high heating rate, however, the apparent activation energy is much lower, implying tar evaporation to be the controlling process [16,17]. Some complex models are difficult to extrapolate to other materials and conditions [23] because the proposed models do not account for the structural and chemical basis. Recently, general models have been developed extending macromolecular network models of coal devolatilization to biomass [7–9]. Despite the fact that biomass devolatilization releases gas and tar, leaving a char residual, similar to coal devolatilization, it is an oversimplification to suggest that the devolatilization of biomass is similar to that of a very low rank coal because significant differences exist between their chemical structures. For instance, coal is predominantly an aromatic material, while in biomass

only lignin has a relatively similar aromatic structure. Niksa [7] and Serio et al. [8,9] based their devolatilization models on such considerations, enabling them to cover a wide range of biomass materials and reaction conditions.

In the present work, a general model for biomass devolatilization is developed. An advanced macromolecular network model of coal devolatilization, the chemical percolation devolatilization (CPD) model developed by Fletcher and coworkers [25–28], was extended to devolatilization of biomass major components based on the consideration of their chemical structure and its transformation under various mechanisms. Although the multicomponent mechanism [9,29,30] is still arguable, previous investigations provided evidence that biomass devolatilization behaves as a superposition of the independent kinetics of the major components [6,9,12,13,29,30].

Model Development

Biomass Components and Their Chemical Structures

Three main chemical components of biomass (i.e., cellulose, hemicellulose and lignin) were considered in the model. Due to the lack of detailed information about the extractives, these were lumped with the less characterized component: hemicellulose. The three components have significantly different chemical structures, which causes their devolatilization characteristics to be significantly different as well [9,11,30].

Cellulose consists of unranked polymers of linked glucose residues arranged in linear chains, where every other glucose residue is rotated approximately by 180°. It has an elemental composition of $C_6H_{10}O_5$ (a single repeating unit of cellulose polymer). Different species of cellulose from different materials and processes have a similar elemental composition and chemical structure, which are very similar to pure cellulose. Cellulose was therefore modeled as a linear molecular chain to determine its structural parameters. The structure of hemicellulose is considered very similar to that of cellulose, but with more branched, shorter chains, and therefore it was also modeled as a linear chain. The chemical structure of lignin is very different from cellulose and is not known exactly, although great progress has been made in that direction (e.g., Ref. [31]). Lignin is a branched polymer of substituted phenyl-propane units joined by carbon-carbon and ether linkages. Lignin structure, monomers combined with linkages, appears random and unorganized, similar to a very simple network low-rank coal structure. There are many possible monomers, and their types and proportions depend on the sources in nature and the processes to obtain it. Compared with low-rank coal, the clusters (e.g., monomers) of lignin are smaller and less cross-linked, resembling a molecular chain cross-linked to form a simple network. Therefore, lignin was modeled as a chain structure, while the cross-linkages were considered through a structural parameter. In summary, the structure of biomass components is more similar to a chain rather than the macromolecular network of low-rank coals. Therefore, to extend the CPD model, a chain structure of biomass components was specified to determine their chemical structural parameters and to model the devolatilization process.

Chemical Structure Parameters

Four chemical parameters are necessary to define the coal chemical structure in the original CPD model, which were directly taken from ^{13}C nuclear magnetic resonance (NMR) measurements [28]. They are (1) the coordination number, $\sigma + 1$, (2) the initial fraction of intact bridges, p_0, (3) the average molecular weight per cluster, MW_1, and (4) the molecular weight per side chain, M_δ. These parameters, that were obtained experimentally for a suite of coals, allow the model to predict the structural transformations during devolatilization without adjusting any model coefficients. For biomass components, however, no NMR data are currently available. In the present work, the parameters were determined based on the assumed chain structure for the components. Two parameters can be fixed simply based on the chain structure. The coordination number ($\sigma + 1$) is 2, because each cluster in a chain has two bridges. Moreover, there is only a small fraction of bridges in the chain extremities, so almost all bridges within a chain are intact, and therefore the initial fraction of intact bridges (p_0) should be 1, but for model application it was set to 0.999. Consequently, only two parameters, MW_1 and M_δ, must be determined for the individual components.

For cellulose, a cluster unit was taken as glucose with molecular weight of 162. The same value was also applied for hemicellulose because of its similar cluster structure. Regarding lignin, there are various types of cluster structures. The expression to calculate the average molecular weight for coal using measured structure parameters [32] was employed to estimate the cluster molecular weight of lignin:

$$MW_1 = (C_{clust} M_C)/(f'_a x_C) \quad (1)$$

where C_{clust} is the number of aromatic carbons per cluster, M_C is the molecular weight of carbon (12 amu), f'_a is the corrected carbon aromaticity (i.e., carbon aromaticity minus carbonyl carbon), and x_C is the percentage of carbon in the coal (on dry ash-free basis). The carbon aromaticity of lignin was reported as 0.67 [33]. Considering lignin structure to be similar to low-rank coals and to have the same

carbonyl carbon fraction (about 0.10 [34]), we use $f'_a = 0.57$ for the calculation. Measurements on lignin structure show that only one aromatic ring is generally contained in most clusters (e.g., Ref. [31]); thus, $C_{clust} = 6$. Consequently, using equation 1, MW_1 can be calculated knowing lignin carbon content. The structure variation then can be taken into account by considering the variation of carbon content in lignin materials.

The size of the side chain, M_δ, of the three components was estimated following the correlation between the final gas yield of devolatilization ($f_{gas,\infty}$) and the cluster structure parameters (MW_1 and M_δ) [28] as follows:

$$f_{gas,\infty} = [m_b(\sigma + 1)(1 - c_0)] \div [2m_a + m_b(\sigma + 1)(1 - c_0)] \quad (2)$$

where m_a is the molecular weight of the cluster and m_b is twice the molecular weight of a side chain, that is,

$$m_a = MW_1 - (\sigma + 1)(M_\delta - 7) \quad (3)$$

$$m_b = 2(M_\delta - 7) \quad (4)$$

From the other structural parameters, M_δ can be obtained from the previous equations. In equation 2, c_0 is also a structural parameter, which denotes the fraction of charred bridges occurring originally in the components. For cellulose and hemicellulose, all bridges are considered labile, therefore, $c_0 = 0$. For lignin, a portion of the bridges was assumed stable accounting for the cross-linking connections. The parameter was fixed to $c_0 = 0.10$ following parameter fitting based on experimental data [21,22]. This assumption implies that the structure cannot be purely chainlike, but this was kept as an approximation.

Devolatilization Reactions and Kinetic Parameters

The model was developed extending the CPD model originally for coal devolatilization to devolatilization of biomass components, which also considers multiple mechanisms, including bridge breaking and rearranging, side-chain cracking and gas release, tar distillation, and cross-linking. The same reaction scheme was applied for biomass as for coals [25,28] although a chainlike structure was taken for the main components:

$$\text{£(labile bridge)} \xrightarrow{k_b} \text{£*(bridge intermediate)}$$

$$\text{£*(bridge intermediate)} \begin{cases} \xrightarrow{k_\delta} 2\delta\ \text{(side chains)} \xrightarrow{k_g} 2g_1\text{(light gases)} \\ \xrightarrow{k_c} \text{c(char bridge)} + 2g_2\text{(light gases)} \end{cases}$$

A simple glucose unit was directly taken as a cluster for cellulose and hemicellulose, while an aromatic ring together with side chains was taken as a cluster for lignin. The exact nature of the bridges and clusters was not specified. The decomposition starts with the breaking of a chemical bond in a labile bridge of a chain to form a highly reactive bridge intermediate. The reactive bridge material may either be released as light gas with the concurrent rearranging of the two associated clusters to give a stable or charred bridge, or else the bridge material may be stabilized to produce side chains from the reactive bridge fragments. The stabilized side chains may be converted eventually into light gases through a subsequent, slower reaction. Statistics were employed to describe the bridge breaking and the size of the fragments formed using the results from Bethe lattices with $\sigma = 1$. Tar is considered as the fragments that evaporate under the distillation mechanism, while the remaining fragments form char. The correlation of tar evaporation from the CPD model was developed [28] for molecular weights ranging from 110 to 315 amu that fit the size of clusters in biomass components.

The present model does not address the volatile composition, but describes the fraction of tars and light-gas species. The side chains attached to the tar fragments evolve as light-gas species in secondary reactions that were assumed to be instantaneous. Therefore, the fraction of side chains in tar is added to the light-gas release during bridge breaking.

The kinetic parameters for the devolatilization reactions, that it, bridge breaking, competitive processes of the bridge intermediates transformations, and light-gas evolution, were fitted for the three components with the literature data, while the kinetic parameters for cross-linking and the correlation coefficients for tar distillation were kept the same as for coals. The model development has been detailed elsewhere [35]. The partitioning of light gases and tar was used for cellulose and lignin to fit the model kinetics, but there is no equivalent data for hemicellulose. The activation energy for gas release from hemicellulose was obtained from mass loss data only at low heating rate [36]. Therefore, the kinetics for this component are not optimized. The resulting kinetic parameters and coefficients are summarized in Table 1 together with the structural parameters of the components.

Modeling Biomass Devolatilization and Biomass Chemical Composition

To extend the model to different biomass types, devolatilization was modeled as a superposition of the behavior of the three components that are described using the parameters fixed in Table 1. The only fuel-specific input to the model is the mass fraction of the components. The determination of the

TABLE 1
The structural parameters and model kinetic parameters of biomass components

Parameter	Cellulose	Hemicellulose	Lignin	Description
Structural parameters				
MW_1	162	162	210[a]; 187[b]	Molecular weight of cluster
M_δ	37	37	42[a], 31[b]	Molecular weight of side chain
Kinetic parameters				
E_b, kcal/mol	59.0	51.5	58.0	Bridge scission activation energy
A_b, s^{-1}	1.0×10^{18}	1.0×10^{18}	1.8×10^{18}	Bridge scission frequency factor
σ_b, kcal/mol	1.8	2.5	6.0	Standard deviation for distribution E_b
E_g, kcal/mol	43.18	38.2	49.0	Gas release activation energy
A_g, s^{-1}	8.23×10^{12}	5.0×10^{12}	5.0×10^{12}	Gas release frequency factor
σ_g, kcal/mol	3.0	5.0	8.0	Standard deviation for distribution E_g
ρ	0.01	0.01	1.0	Frequency factor ratio of two pathways
E_c, kcal/mol	−6.6	−4.9	0	Activation energy difference between two pathways
E_{cross}, kcal/mol	65.0	65.0	65.0	Cross-linking activation energy
A_{cross}, s^{-1}	3×10^{15}	3×10^{15}	3×10^{15}	Cross-linking frequency factor

[a] For woody lignin.
[b] For herbaceous lignin.

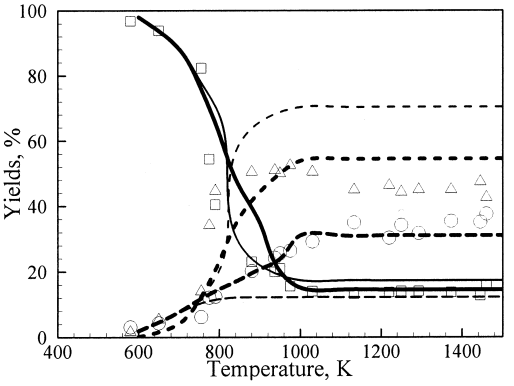

FIG. 1. Model prediction compared with measured data of lignin devolatilization at high heating rate (1000 K/s) [21]. The symbols denote the measured values: char, □; tar, △; light gases, ○. The curves are model predictions (coarse curves: prediction with consideration of secondary reaction; fine curves: prediction without consideration of secondary reaction.): char, solid curve (—); tar, shorter-dashed curve (---); light gases, longer-dashed curve (––).

composition is more complex than the usual proximate and ultimate analyses, so a correlation was developed based on literature data [9] to express the mass fractions of cellulose and lignin as a function of the oxygen and hydrogen to carbon atomic ratio (O/C and H/C) in biomass and the volatile matter (VM) in weight percent daf, in the form

$$\begin{aligned}\text{cellulose} = &-1019.07 + 293.810\,(\text{O/C}) \\ &- 187.639\,(\text{O/C})^2 + 65.1426\,(\text{H/C}) \\ &- 19.3025\,(\text{H/C})^2 + 21.7448\,(\text{VM}) \\ &- 0.132123\,(\text{VM})^2 \end{aligned} \quad (5)$$

$$\begin{aligned}\text{lignin} = &\ 612.099 + 195.366\,(\text{O/C}) \\ &- 156.535\,(\text{O/C})^2 + 511.357\,(\text{H/C}) \\ &- 177.025\,(\text{H/C})^2 - 24.3224\,(\text{VM}) \\ &+ 0.145306\,(\text{VM})^2 \end{aligned} \quad (6)$$

The correlation was developed for a large range of biomass samples with molar ratios O/C from 0.56 to 0.83, H/C from 1.26 to 1.69, and VM from 73 to 86% daf. The correlation coefficient for cellulose is 90%, while for lignin is 81%; it is thus acceptable for use but leaves room for improvement [35].

Results and Discussion

Using the structural parameters and the fitted kinetic parameters, the model has been extensively validated and applied to the experimental data on devolatilization of cellulose [9,15,17,30], hemicellulose (hemicellulose and xylan) [9,30], and lignin [9,21,22,30]. The model validation for the components' devolatilization is detailed in Ref. [35]. The comparison of the model prediction with the measurement on lignin devolatilization at high heating rate (1000 K/s) [21] is shown as an example in Fig. 1. It can be found that the model can reasonably

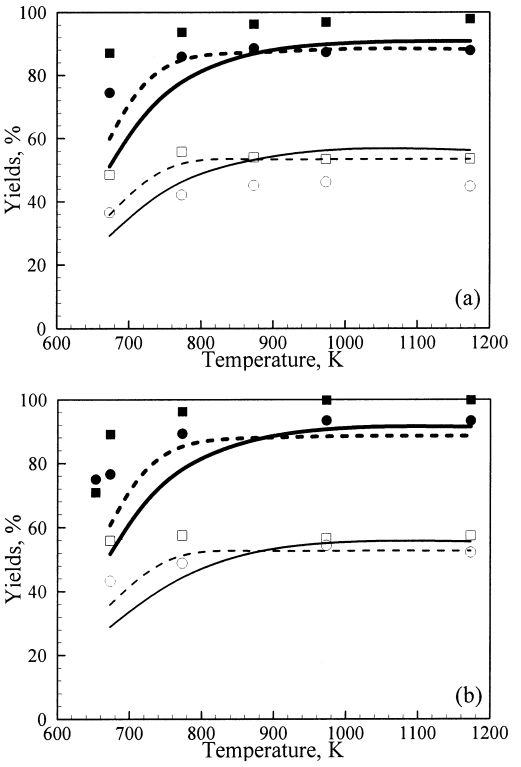

FIG. 2. Model prediction compared with experimental values [37]: (a) sugar-cane bagasse, (b) silver birch. Heating rates are indicated in the legend, and the holding time is 30 s. The symbols denote the measured data. Total volatile yield: ■, 1000 K/s; ●, 1 K/s. Tar yield: □, 1000 K/s; ○, 1 K/s. The curves denote model calculations. Total volatile yield: coarse solid curve, 1000 K/s; coarse dashed curve, 1 K/s. Tar yield: fine solid curve, 1000 K/s; fine dashed curve, 1 K/s.

represent the devolatilization of lignin at high heating rate and reproduce well the yields of light gases, tar, as well as char as a function of devolatilization temperature. The model validation shows that the model can not only be applied to the devolatilization of biomass components from different resources, but also covering a wide range of reaction conditions such as heating rate [35].

Devolatilization in practical firing processes generally takes place at high heating rate and high temperature, when tar evaporation and mass transportation play a predominant role [16,17]. The volatiles, particularly tar, may undergo further reactions, and therefore small particle size and special design of experimental apparatus were commonly employed in the measurements to mitigate such effects (e.g., Nunn et al. [10]). Although biomass devolatilization occurs at relatively low temperature, for high heating rate secondary reactions may still be important at high temperatures around the particle. For example, Hajaligol et al. [15] and Nunn et al. [10,21] indicated that secondary reactions occurred in their electrical screen heater reactor, leading to the measured tar yield decreasing and gas yield increasing for temperatures higher than 800 K. In the original CPD model for coals, secondary reactions were excluded considering an approximate normalization procedure by the tar yield [25,28]. When this is applied for biomass devolatilization, the tar yield is significantly overestimated for temperatures higher than 800 K (see Fig. 1). Therefore, the effect of secondary reactions should be included so that the model can be applicable to practical processes. Compared with coals, the smaller clusters and easy bridge breaking result in smaller fragments generated from biomass, which evaporate easily as tar but perhaps still contain a considerable number of side chains. The further release of side chains attached to evaporated tar was considered, which allows the model to predict reasonably the gas yield and the tar yield (see Fig. 1). Even so, the model still underpredicts the gas yield and does not predict the decrease in tar yield, which perhaps is an indication that the clusters in tar may further decompose into light gases.

After the reaction mechanisms and kinetic parameters for the three components are fully specified, the model can be applied to the devolatilization of various biomass types based on the multicomponent mechanism. The mass fraction can be measured or determined with the proposed correlation (equations 5 and 6). The model predictions were compared with the measured yields of devolatilization products reported for different biomass devolatilizing under different conditions, particularly under high heating rates of interest to practical combustion process. Sample results are shown in Figs. 2 and 3. For Fig. 2, the components' composition was directly taken from the measurement, that is, bagasse contains 79% cellulose and hemicellulose modeled as cellulose and 21% lignin, and silver birch contains 61% cellulose, 19% hemicellulose, and 20% lignin [37]. For these two biomass materials, the comparison (see Fig. 2) indicates that the model can reasonably reproduce the yields of total volatiles and tar and the variation with temperature. At low temperatures, the model underpredicts the yields at both heating rates, which may be attributed to the cooling stage that is not simulated. Additionally, the model predicts the higher yields at lower heating rate since the devolatilization occurs mainly at the higher temperature. At high temperature, the model predicts the increase of tar yield at an intermediate level compared to both measurements. The char yield is overpredicted at high heating rate.

Although the lignin content of the two biomasses considered is similar, the measured devolatilization yields are different. The model considers two types

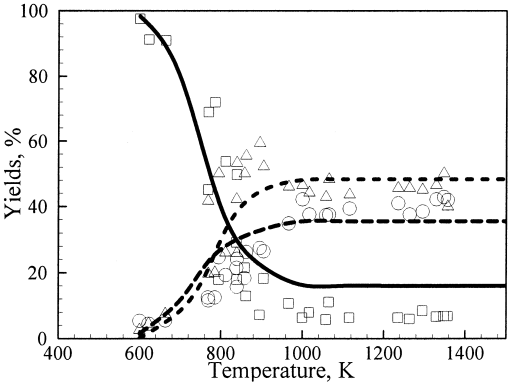

FIG. 3. Model prediction compared with measured devolatilization of sweet gum hardwood at heating rate of 1000 K/s [10]. The symbols denote the measured values: char, □; tar, △, light gases, ○. The curves are model predictions: char, solid curve (—); tar, shorter-dashed curve (---); light gases, longer-dashed curve (––).

of lignin depending on the type of biomass that was classified in two groups, woody lignin and herbaceous lignin, and two sets of structural parameters were set for the two groups respectively (see Table 1). For the calculation in Fig. 2, woody lignin was applied to silver birch and the herbaceous lignin was applied to bagasse. Woody biomass generally has a higher lignin content and produces more volatiles from devolatilization experiments and also from proximate analysis. Therefore, higher molecular weights for the cluster and side chain were set for woody lignin to represent the more ordered structure of woody materials producing more volatiles.

The model predictions are also compared with the experimental data of sweet gum hardwood devolatilization at a 1000 K/s heating rate (see Fig. 3). For this hardwood, no chemical composition was reported in Ref. [10], so the mass fraction of main components was calculated with the proposed empirical correlation, leading to 41.6% cellulose, 24.1% lignin, and 34.2% hemicellulose (including extractives). With the calculated composition, it can be found that the model can represent well the yields of char, tar, and light gas as a function of peak temperature. This test verifies not only the application of the model but also the reliability of the empirical correlation. The overprediction of char yield at high temperatures can be attributed to the hemicellulose model, which needs improvement with detailed tar and gas release measurements.

The most important inputs for the model are the chemical structure parameters. The consideration of a chain structure for cellulose and chainlike structure assumed for hemicellulose and lignin allowed an empirical estimate of these parameters. For lignin, such an assumption may be arguable because it is generally considered as a network similar to low-rank coals. Even so, previous models of the lignin molecule (e.g., Ref. [31]) have shown that the network is very simple and most of the clusters are arranged in chains while the chains are connected each other with cross-linking. The smaller clusters are easily broken from the network whether they are in chains or in cross-linking. Model validation of devolatilization of various lignins under different conditions confirms that the chain assumption may not lead to a significant effect on the modeling results. Niksa also applied the assumption of chain structure to develop the FLASHCHAIN model for biomass and even for coals [7]. The estimated molecular weight of clusters of cellulose, hemicellulose, and lignin based on the chain structure assumption are consistent with the field ionization mass spectrometry measured average molecular weight of the potential species evolving during devolatilization of these components as well as biomass [9,22]. Moreover, the correlation of tar evaporation [25,28] well describing the tar release also verifies the estimated cluster molecular weight of biomass components.

Conclusions

In the present work, the CPD model originally developed for coal devolatilization was extended to devolatilization of biomass components, that is, cellulose, hemicellulose, and lignin. The reaction scheme considered for coals was applied for these components. The model also considers the multiple mechanisms of the global devolatilization reaction, including bridge breaking, bridge rearrangement, side-chain cracking and gas release, tar distillation, and cross-linking. Model modifications were performed based on the specific structure of the components. Moreover, secondary reaction of tar containing side chains was included and was particularly important for devolatilization at high temperature and high heating rates. Biomass devolatilization kinetics were modeled as a superposition of the independent kinetics of the three main components. The structural and kinetic parameters for the components were fixed. The only fuel-specific input is the chemical composition, which comes from measured data or can be estimated with an empirical correlation of chemical composition and the conventional proximate and ultimate analyses. The results show that the model successfully describes the devolatilization of various biomass samples, particularly at high heating rate.

Acknowledgments

Support from the European Commission ENERGIE Programme under contract Bioflam ENK5-1999-00004 is acknowledged, and a research scholarship from PRAXIS

XXI/BPD/20160/99 of FCT (Fundacão para a Ciência e a Tecnologia) of the Ministry of Science and Technology of Portugal to Dr. C.-D. Sheng is also appreciated.

REFERENCES

1. Werther, J., Saenger, M., Hartge, E.-U., Ogada, T., and Siagi, Z., *Prog. Energy Combust. Sci.* 26:1–27 (2000).
2. Antal, M. J., in *Advances in Solar Energy* (K. W. Boer and J. A. Duffie, eds.), American Solar Energy Society, Plenum Press, New York, 1985, pp. 175–255.
3. Shafizadeh, F., "The Chemistry of Solid Wood," in *Advances in Chemistry* Series No. 207 (R. W. Rowell, ed.), American Chemical Society, Washington, DC, 1984.
4. Elliott, D. C., Beckman, D., Bridgwater, A. V., Diebold, J. P., Gevert, S. B., and Slantausta, Y., *Energy Fuels* 5:399–400 (1991).
5. Bridgwater, A. V., and Cottam, M.-L., *Energy Fuels* 6:113–120 (1992).
6. Roberts, A. F., *Combust. Flame* 14:261–272 (1970).
7. Niksa, S., *Proc. Combust. Inst.* 28:2727–2733 (2000).
8. Chen, Y., Charpenay, S., Jensen, A., Wójtowicz, M. A., and Serio, M. A., *Proc. Combust. Inst.* 27:1327–1334 (1998).
9. Serio, M. A., Wójtowicz, M. A., Chen, Y., Charpenay, S., Jensen, A., Bassilakis, R., and Riek, K., *A Comprehensive Model of Biomass Pyrolysis,* final report for USDA Contract 96-33610-2675, Advanced Fuel Research Inc., East Hartford, CT, 1997.
10. Nunn, T. R., Howard, J. B., Longwell, J. P., and Peters, W. A., *Ind. Eng. Chem. Process Des. Dev.* 24:836–844 (1985).
11. Órfão, J. J. M., Antunes, F. J. A., and Figueiredo, J. L., *Fuel* 78:349–358 (1999).
12. Ward, S. M., and Braslaw, J., *Combust. Flame* 61:261–269 (1985).
13. Miller, R. S., and Bellan, J., *Combust. Sci. Technol.* 126:97–137 (1997).
14. Lewellen, P. C., Peters, W. A., and Howard, J. B., *Proc. Combust. Inst.* 16:1471–1480 (1976).
15. Hajaligol, M. R., Howard, J. B., Longwell, J. P., and Peters, W. A., *Ind. Eng. Chem. Process Des. Dev.* 21:457–465 (1981).
16. Suuberg, E. M., Milosavljevic, I., and Oja, V., *Proc. Combust. Inst.* 26:1515–1527 (1996).
17. Milosavljevic, I., and Suuberg, E. M., *Ind. Eng. Chem. Res.* 34:1081–1097 (1995).
18. Di Blasi, C., *Biomass Bioenergy* 7:87–98 (1994).
19. Petrocelli, E. P., and Klein, M. T., in *Fundamentals of Thermochemical Biomass Conversion* (R. P. Overend, T. A. Milne, and L. K. Mudge, eds.), Elsevier, New York, 1985, pp. 257–273.
20. Train, P. M., and Klein, M. T., in *Pyrolysis Oils from Biomass,* ACS Symposium Series 376 (E. J. Soltes and T. A. Milne, eds.), American Chemical Society, Washington, DC, 1988, pp. 241–263.
21. Nunn, T. R., Howard, J. B., Longwell, J. P., and Peters, W. A., *Ind. Eng. Chem. Process Des. Dev.* 24:844–852 (1985).
22. Serio, M. A., Charpenay, S., Bassilakis, R., and Solomon, P. R., *Biomass Bioenergy* 7:107–124 (1994).
23. Di Blasi, C., *Prog. Energy Combust. Sci.* 19:71–104 (1993).
24. Antal Jr., M. J., and Varhegyi, G., *Ind. Eng. Chem. Res.* 34:703–717 (1995).
25. Grant, D. M., Pugmire, R. J., Fletcher, T. H., and Kerstein, A. R., *Energy Fuels* 3:175–186 (1989).
26. Fletcher, T. H., Kerstein, A. R., Pugmire, R. J., and Grant, D. M., *Energy Fuels* 4:54–60 (1990).
27. Fletcher, T. H., Kerstein, A. R., Pugmire, R. J., and Grant, D. M., *Energy Fuels* 6:414–421 (1992).
28. Fletcher, T. H., Kerstein, A. R., Pugmire, R. J., Solum, M., and Grant, D. M., A *Chemical Percolation Model for Devolatilization: Summary,* Sandia report SAND 92-8207.
29. Evans, R. J., and Milne, T. A., *Energy Fuels* 1:123–137 (1987).
30. Raveendran, K., Ganesh, A., and Khilar, K. C., *Fuel* 75:987–998 (1996).
31. Brunow, G., Kilpeläinen, I., Sipilä, J., Syrjänen, K., Karhunen, P., Setälä, H., and Rummakko, P., in *Lignin and Lignan Biosynthesis,* ACS Symposium Series 697 (N. G. Lewis and S. Sarkanen, eds.), American Chemical Society, Washington, DC, 1998, pp. 131–147.
32. Solum, M. S., Pugmire, R. J., and Grand, D. M., *Energy Fuels* 3:187–193 (1989).
33. Hagaman, E. W., and Lee, S. K., *Prepr. Pap.—Am. Chem. Soc., Div. Fuel Chem.* 42:244–247 (1997).
34. Smith, K. L., Smoot, L. D., and Fletcher, T. F., in *Fundamentals of Coal Combustion* (L. D. Smoot, ed.), Elsevier, New York, 1993, pp. 131–298.
35. Sheng, C., and Azevedo, J. L. T., *Mathematical Description of Specific Secondary Fuel Phenomena in Pulverized Coal Flames,* Research report of BioFlam project, Instituto Superior Tecnico, Lisbon, Portugal, 2001.
36. Vohegyi, G., and Antal, J. M., *Energy Fuels* 3:329–335 (1989).
37. Fraga, A.-R., Gaines, A. F., and Kandiyoti, R., *Fuel* 70:803–809 (1991).

COMMENTS

Matthias Mueller-Hagedorn, University of Karlsruhe, Germany. You divided the lignin into two groups (herbaceous/woody); why did you not do it also in the case of hemicelluloses? In deciduous trees, the hemicelluloses are built up largely of xylose monomers (it's a C5 sugar), so the monomer mass should be 132 instead of 162. In my opinion, the division of lignin into herbaceous and woody is not significant. By means of your monomer masses you divided into guaiacol and syringol derivatives (+ ca. 30 amu).

Author's Reply. We divided the lignin in two groups because we had high heating rate data available for both types of lignin. We think that this is not essential because the differences between the two types of lignin are small, as can be seen from the model results. Regarding hemicellulose, as we stressed in the paper, there is no data available on high heating rate devolatilization; therefore, we could not propose parameters with confidence for this component and we could not differentiate different types.

We recognize that hemicelluloses contain a large fraction of xylose monomers, although they also include other monomers with smaller and higher molecular weights. From the molecular model (Ref. [9] in paper), the molecular weight per monomer is about 160 atomic molecular units, so we think our assumption is reasonable. With more data available for hemicellulose, we think the model may be improved, based on other values of the monomer molecular weight. We kept the molecular mass close to cellulose due to the shortage of devolatilization data.

The monomer masses for lignin were not specified from their chemical structure because we did not have data available, so we used the carbon mass fraction to estimate this value. We appreciate your observation that the difference between the monomers masses we obtained (Ref. [23] in paper) may correspond to a larger fraction of syringol rather than guaiacol derivates in the woody lignin, although we do not have data to show it.